International Scholars Journals

International Journal of Education Research and Reviews ISSN 2329-9843 Vol. 7 (4), pp. 001-006, April, 2019. Available online at www.internationalscholarsjournals.org © International Scholars Journals

Review

Upper mantle velocity structure in the NW Himalaya: Hindu Kush to Garhwal region from travel time studies of deep Hindu Kush earthquakes

Sushil Kumar[1*], R. Chander[2] and K. N. Khattri[3]

[1]Scientist (Seismologist), Wadia Institute of Himalayan Geology, P.B.No.74, Dehra Dun –248 001(UA), India.
[2]I.I.T. Roorkee, Roorkee, formerly University of Roorkee), 290, Sector 4, Mansadevi complex, Panchkula – 134109, Haryana, India.
[3]I.I.T. Roorkee, Roorkee, formerly University of Roorkee), 100 Rajender Nagar, Dehra Dun-248001 (UA) India.

Accepted 09 January, 2019

The 22 Hindu Kush earthquakes had focal depths in the range of 50 to 245 km approximately. The 154 P travel time readings obtained from them were interpreted using a computer program based on least squared inversion and written specifically for the purpose. The upper mantle P- wave velocity along the north-west Himalaya obtained from this study has a value of 8.1 km/s. It appear to persist up to a depth of about 100 km below that level, it appears to increase to 8.35 km/s. The upper mantle P- wave velocity is found to be comparable to that obtained along a DSS profile in Kashmir. However, it is lower by 0.35 km/s from the value estimated by Ni and Barazangi in 1982.

Key words: NW Himalaya, P travel time, upper mantle structure, Hindu Kush to Garhwal Himalaya.

INTRODUCTION

Among the various geophysical techniques, so far seismology has provided the most detailed information about the internal structure of the earth. Initially, chronometric information about the travel times of seismic body waves, dispersion of surface waves and periods of peaks in Fourier spectra of free oscillations of the earth were analyzed for the purpose. However, more recently, infor-mation about amplitudes of recorded seismic waves has been utilized also. Analysis of body wave travel times yield information about spatial distribution of compres-sional (V_p) and shear (V_s) wave velocities within the earth.

In the past few decades the inversion of travel time data for wave velocity distribution in the earth using the ray tracing approach has been formulated as a program-ing problem and many ingenious but rigorous techniques have been employed (Aki and Richards, 1980). However, the quality and quantity of the data at our disposal constrain us to evolve a simpler strategy for a limited goal. Thus, we still solve a programming problem but estimate only two parameters at a time, namely, the magnitude of V_p in the deepest layer of a multi layered earth and the depth of the top boundary of this layer.

In this study, we have analyzed the travel times of seismic P waves from Hindu Kush earthquake recorded at temporary seismograph stations in the Garhwal Himalaya (Figure 1). The aperture of the seismograph array in Garhwal was about 40 km. We adopt the hypocentral location and origin times of the concerned earthquakes as reported by the US geological survey to obtain the necessary travel times. The epicenters of the Hindu Kush earthquakes whose data are analyzed were clustered in a 100 km by 50 km area. The focal depth of these earthquakes as estimated by the USGS ranged between 50 to 250 km approximately. Thus for a very short range of epicentral distances we had travel time information about rays traversing the upper mantle at several depths in the 50 to 245 km range.

It was observed through ray tracing that these rays pass through the crust only once near the recording station. Moreover, their travel time through the crust is a relatively small fraction of the total travel time. Hence, distribution of V_p in the crust was not investigated. However, an average crustal model was assumed to obtained estimates of V_p in the upper mantle.

*Corresponding author. E-mail: sushil_rohella@hotmail.com. Fax: 0135-2625212(o). Phone: +91-09897220017(m).

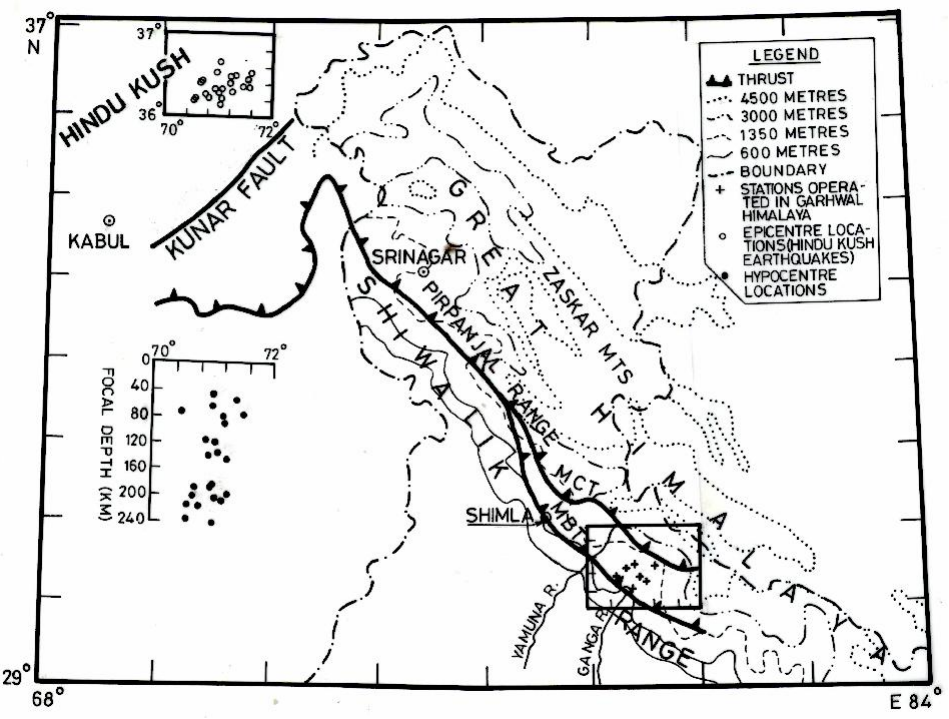

Figure 1. North-Western Himalaya with epicenters of Hindu Kush earthquakes and stations of recording array in Garhwal Himalaya.

Table 1. Roecker's model of P wave speed for the Hindu Kush region.

Roecker (1982)	
Depth (km)	**P-wave speed (km/s)**
00 – 40	5.80
40 – 70	6.40
70 – 110	8.05
110 – 160	8.50
160 – 185	8.30
185 – 230	9.10

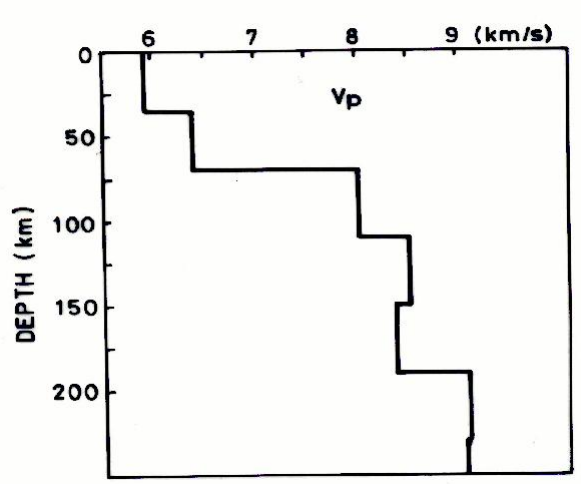

Figure 2. Wave speed model for Hindu Kush according to Roecker (1982).

Roecker (1982) determined a detailed V_p structure under the Hindu Kush mountains up to a depth of about 200 km. This was an elaborate exercise using locally record-ed P wave data. We take account of Roecker's (1982) results in our estimations of upper mantle V_p values. In this way, we feel justified in claiming that we have exa-mined V_p distribution in the upper mantle the NW Hima-laya (Figure 1).

Review of wave velocity determinations based on data for Hindu Kush earthquakes

Earthquakes of the Hindu Kush region have attracted attention of seismologists for many years. A number of wave velocity determinations have been made using re-corded phases from these earthquakes (Roecker, 1982; Tandon 1967; Matveyeva and Lukk, 1968; Kaila et al., 1969; Ram and Mereu, 1977) . These studies fall into two distinct categories. The work of Roecker (1982) is differ-rent from those of others in that seismographs were installled at very short epicentral distances within the Hindu Kush region of Afghanistan. Thus, the wave velo-

Table 2. Comparison of P- wave speed models deduced by various investigators using Hindu Kush data.

Kaila et al. (1969)		Matveyeva and Lukk (1968)		Tandon (1967)		Ram and Mereu (1977)	
Depth (km)	P-wave speed (km/s)	Depth (km)	P-wave speed (km/s)	Depth (km)	P-wave speed (km/s)	Depth (km)	P-wave speed (km/s)
45	8.14	00	5.90	31.85	8.01	15	5.50
70	8.32	50	6.10-7.90	63.71	8.03	33	6.50
85	8.29	80	8.00-8.35	95.56	8.02	113	7.90
100	8.30	110	8.05-8.36	127.40	8.07	362	8.13
120	8.37	150	8.20-8.35	159.27	8.40	545	9.67
150	8.39	200	8.37-8.54	191.13	8.45	-	-
190	8.53	390	8.54-8.71	-	-	-	-
210	8.35	-	-	-	-	-	-
230	8.57	-	-	-	-	-	-

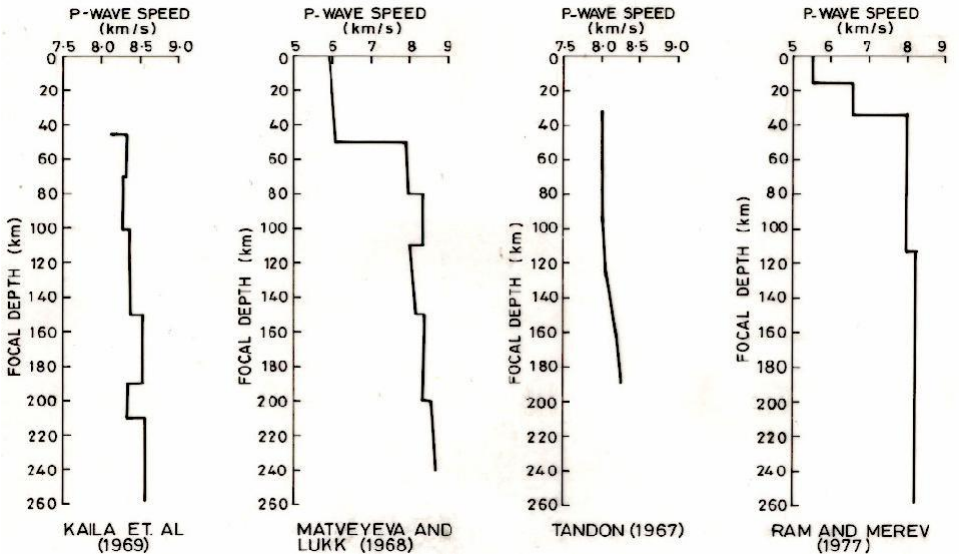

Figure 3. Comparison of wave speed models deduced by various Investigators using Hindu Kush earthquake data.

city determination applies to the Hindu Kush region strictly. Table 1 and Figure 2 are displays representing their initial, laterally homogeneous model determined for the region. Subsequently, they estimated lateral variations of up to few percent of the average V_p at a given level in the region. Thus, the results do not strictly apply to a specific region. Still a comparison of the result is given in Table 2 and Figure 3. This is because while our study also belongs to the latter category, still it has the distinction that essentially one path is investigated (Table 1 and 2, Figures 2 and 3)

Observations

General

During 1985 - 1986, many earthquakes occurring in the Hindu Kush region were picked up by the portable recording stations installed in the Garhwal Himalaya for local seismicity studies. We analyze here the P wave readings obtained from seismograms of the seven stations. Records of 22 Hindu Kush earthquakes were found to have readable P phases on these seismograms. The hypocentral information about these earthquakes as determined by the US Geological survey is given in Table 3. As seen from this table, the distribution of the focal depth of the 22 earthquakes is not uniform. There is notable lack of earthquakes from the depths ranges of 94 to 117 km and 142 to 188 km.

Travel times graphs

Table 4 is a display of the arrival times of P phases at different stations of the array for these earthquakes.

Table 3. Hypocentral data of 22 earthquakes.

S. No.	Date			Origin Time			Magnitude	Epicenter		Focal depth
	Mon	Day	Year	Hr	Min	Sec	Mb	Lat ^{o}N	Long ^{o}E	(km)
1	Dec	22	1985	07	32	17.82	4.8	36.331	70.992	49.7
2	Nov	29	1985	10	10	03.64	5.0	36.404	71.409	57.4
3	Dec	26	1985	13	46	22.00	4.2	36.301	71.001	65.6
4	Feb	24	1986	05	57	29.37	5.0	36.086	70.479	77.1
5	Jan	30	1986	09	44	43.00	4.6	36.387	71.512	78.7
6	Nov	26	1985	10	31	08.68	4.7	36.437	71.196	92.2
7	Feb	23	1986	06	50	02.84	4.5	36.336	71.234	93.7
8	May	29	1986	01	30	31.89	4.9	36.288	70.860	116.9
9	Feb	11	1986	12	44	24.26	4.9	36.372	70.910	118.8
10	Dec	15	1985	00	15	29.18	4.5	36.188	71.039	119.2
11	Dec	23	1985	23	26	34.97	4.8	36.241	71.064	120.6
12	May	24	1986	02	01	57.73	4.6	36.367	70.957	141.8
13	Dec	14	1985	07	55	49.99	4.2	36.683	71.014	184.6
14	Dec	06	1985	12	34	41.44	4.7	36.564	70.981	188.2
15	May	25	1986	17	08	56.85	4.4	36.465	70.720	189.2
16	Mar	10	1986	07	41	29.95	4.2	36.532	71.265	199.7
17	Feb	05	1986	01	13	56.69	4.8	36.426	70.696	202.7
18	Jan	11	1986	02	43	03.37	4.3	36.370	71.067	204.2
19	Mar	11	1986	20	39	19.48	4.7	36.512	71.187	207.8
20	Mar	07	1986	02	45	28.51	4.4	36.314	70.789	218.0
21	Nov	22	1985	13	14	55.04	3.8	36.236	70.576	238.1
22	Jan	14	1986	08	33	37.46	5.2	36.341	71.024	245.1

Table 4. Arrival times at different stations from 22 earthquakes listed in table 3.

Event	Date			Nearest arrival time		AKM	CHA	BNA	ODA	DAG	TIL	UKH
	Mon	Day	Year	Hr	Min	Sec	Sec	Sec	Sec	Sec	Sec	Sec
1.	Dec	22	1985	07	32	25.00	24.00	25.90	28.50	28.40	29.20	30.00
2.	Nov	29	1985	10	10	07.10	07.00	08.00	10.30	11.30	11.60	-
3.	Dec	26	1985	13	46	27.00	26.10	28.00	30.30	30.40	31.70	-
4.	Feb	24	1986	05	57	35.90	35.80	37.20	39.00	39.00	40.15	40.30
5.	Jan	30	1986	09	44	44.20	44.20	45.60	47.40	47.60	47.40	48.80
6.	Nov	26	1985	10	31	13.00	14.00	14.30	16.20	17.00	16.90	17.90
7.	Feb	23	1986	06	50	07.00	06.40	07.80	09.50	10.00	10.75	11.00
8.	May	29	1986	01	30	36.00	-	37.60	39.40	40.00	40.80	41.30
9.	Feb	11	1986	12	44	28.30	-	29.20	31.30	31.70	32.40	32.60
10.	Dec	15	1985	00	15	29.80	30.50	32.00	33.90	34.50	35.00	35.40
11.	Dec	23	1985	23	26	36.00	36.00	-	38.90	39.00	35.00	37.00
12.	May	24	1986	02	01	-	-	05.00	06.40	07.00	07.90	08.60
13.	Dec	14	1985	07	55	57.00	57.05	07.80	60.20	60.00	60.90	61.32
14.	Dec	06	1985	12	34	45.00	45.60	46.00	48.00	49.54	08.90	49.80
15.	May	25	1986	17	08	-	-	-	-	04.50	05.50	06.40
16.	Mar	10	1986	07	41	-	31.20	32.50	34.00	33.30	34.60	35.30
17.	Feb	05	1986	01	13	01.30	01.20	02.50	04.40	04.00	05.30	05.40
18.	Jan	11	1986	02	43	05.20	05.10	06.40	08.00	08.60	09.10	09.10
19.	Mar	11	1986	20	39	20.90	20.20	21.50	24.40	24.70	24.10	24.85
20.	Mar	07	1986	02	45	32.00	31.20	32.40	-	34.00	35.50	35.60
21.	Nov	22	1985	13	14	58.80	59.00	60.40	-	63.00	62.50	63.70
22.	Jan	14	1986	08	33	38.20	38.50	39.40	41.70	42.00	42.00	42.70

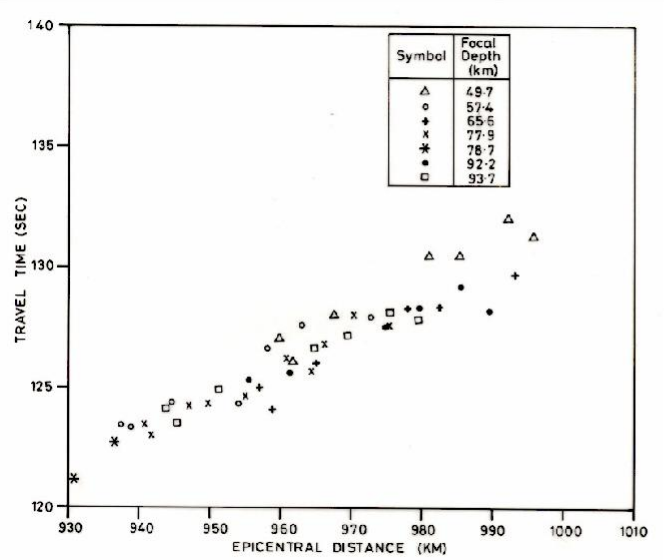

Figure 4. Travel time data for I earthquake cluster.

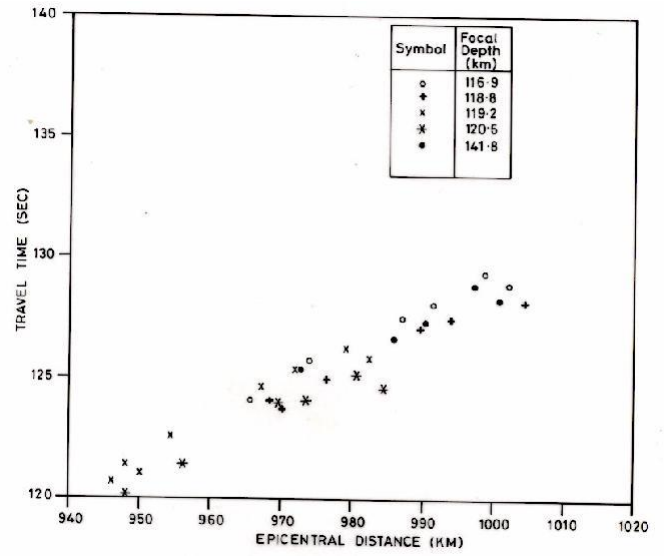

Figure 5. Travel time data for II earthquake cluster.

Using the reported epicentral coordinates of the earthquakes, 154 (22 earthquakes x 7 stations) epicentral distances were computed using the standard formula (Bullen and Bolt, 1985). Corresponding travel times were obtained using the USGS determined origin times for these 22 earthquakes and the respective P wave arrival times. The estimated travel times are plotted for the earthquakes arranged according to the clustering of depths ranges of the concerned earthquakes (Figures 4 to 6). There is a definite gradation in the travel times according to the depth of the earthquakes. Deeper earthquakes yield lesser travel times overall. Figure 1 is a combined display of epicentral locations and the record-

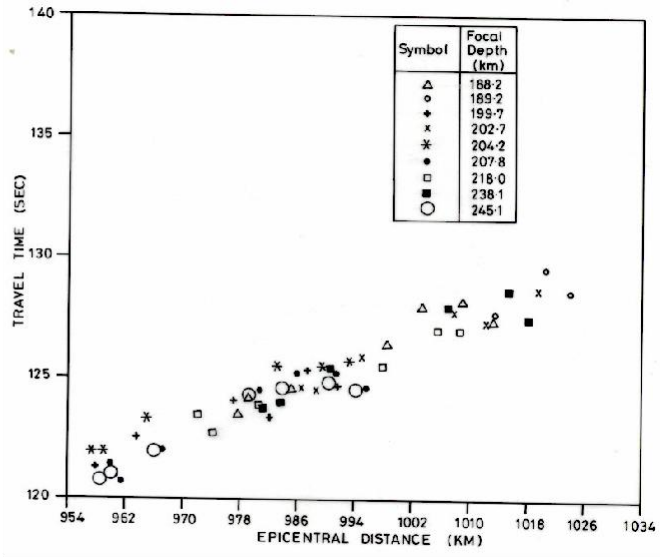

Figure 6. Travel time data for III earthquake cluster.

the recording array against the backdrop of a geological map of the Himalaya. It is seen that the great circles between epicenters and recording stations lie mostly in the NW Outer and Lesser Himalaya.

Method of interpretation of travel times

The method of interpretation adopted by us for the above data is the result of a conscious decision in view of anumber of factors. Firstly, the number of observation is small. This has been governed by the number of readable seismograms obtained during the limited period of array operation. In addition, the number of stations operating was only seven. Secondly, because of concentration of epicenters in a narrow geographic region and the small aperture of the array, the range of epicentral distances covered is too narrow. Thirdly, the observations are subject to considerable errors, which are difficult to quantify.

On a different note, a ray tracing exercise revealed that the travel times of the rays through the crust would be a small fraction of the total travel time. Therefore, we decided to include an average crust with a single layer of average P wave velocity in the models.

Finally, clustering in focal depths among the concerned earthquakes suggested that inversion for upper mantle P wave velocity could be carried out sequentially, starting with the group of earthquakes with the shallowest hypocenters to determine P wave velocity in the upper most mantle layer. Then the next group of earthquakes could be used to investigate the next depths range in the upper mantle. Thus, at the most two parameters would be estimated using a comparatively large number of travel time observations at every step of the sequence. These parameters would be in each case layer P wave veloci-

ty (V_P) and the depth of the top interface of the layer.

The travel time inversion algorithm

Estimation of wave velocity in the last layer of a layered model

Let there be a stack of *L* homogeneous layers with parallel interfaces. Let P wave velocity in the top *L*- 1 layer be specified along with their thicknesses. Let m earth-quakes with known hypocentral coordinates occur in the *L* th layer. Also, let the arrival times of P waves at n seismograph stations be known along with their coordinates. Then the estimation of V_{Pl} (the V_P in the *L* th layer) can be set up as a least squares inversion problem. Let T_{oi} and T_{ci} stand for observed and theoretically computed travel times for the / th ray among the totality of m x n rays between m earthquakes and n stations. The error function E (V_{pl}) is given by

$$E(V_{pl}) = \sum_{i=1}^{mn} (T_{oici} - T(V_{pl}))^2 \quad \ldots (1)$$

If *j* is the running index for layer numbers then,

$$T_{ci}(V_{pl}) = \sum_{j=1}^{l} \frac{L_{ij}}{V_{pj}} \quad \ldots (2)$$

Where, L_{ij} and V_{pj} are the segment length of *L* th ray and P wave velocity in the *J*th layer respectively.
We seek a value of V_{pl} to minimize E (V_{pl}). In other words,

$$\frac{\partial E(V_{pl})}{\partial V_{pl}} = 0 \quad \ldots (3)$$

Equation (3) is non- linear in V_{pl}.. We used the Newton-Raphson procedure to solve this equation iteratively for V_{pl} . Thus, let us define

$$F(V_{pl}) = \frac{\partial E}{\partial V_{pl}} \quad \ldots (4)$$

For brevity Let V_{pl1} be an initial guess of V_{pl}. Let h be an increment V_{pl1} such that

$$F(V_{pl1} + h) = 0 \quad \ldots (5)$$

Expanding F in a Taylor series and retaining only the first two terms, we may write that

$$h = -\frac{F(V_{pl})}{\frac{\partial F}{\partial V_{pl}}\Big|_{Vpl1}} \quad \ldots (6)$$

Or, in terms of the original error function,

$$h = -\frac{\frac{\partial E}{\partial V_{pl}}}{\frac{\partial V^2{}_{pl}}{\partial V^2{}_{pl}}\Big|_{Vpl1}} \quad \ldots (7)$$

Hence, a better guess of V_{pl} is obtained as V_{pl1} + h. The procedure can then be repeated until h becomes negligibly small. The last value of V_{pl1} + h can be taken as an estimate of V_{pl}.

Three dimensional ray tracing

The above iterative scheme to determine V_{pl} cannot be implemented without an accompanying algorithm to trace a ray between specified positions of the hypocenters and the recording stations. The need for three-dimensional ray tracing was visualized for the following reason. We were prepared to simulate and structure under the NW Himalaya through models with parallel uniform layers because of the absence of sufficient other information to constrain a three dimensional visualization of the distribution of V_p in the region of interest. Still, Roecker (1982) had published a three dimensional model of V_p distribution in the Hindu Kush mountains. The model is quite different from world average models of V_{pl} in the upper mantle such as PREM (Bullen and Bolt, 1985). If Roecker's model were to be meshed with the parallel layer model for the rest of the path, then this would have to be through three-dimensional ray tracing.

A shooting strategy was adopted to trace the desired ray iteratively in specified models of V_p. A number of ray tracing formulation are available in the literature (Shah, 1973; Sorerells et al., 1971; Chander, 1977). We adopted the formulation of Sorrels et al. (1971) because of its generality. A computer program was written for the purpose and thoroughly tested.

Computer program

An original program to solve Equation (3) using Equation (4) was written in FORTRAN code. The program was tested thoroughly on synthetic data and then put into use to interpret the travel time observations.

Grid search for estimation of the depth to top interface of the *L* th layer

A grid search strategy was adopted for this purpose. The

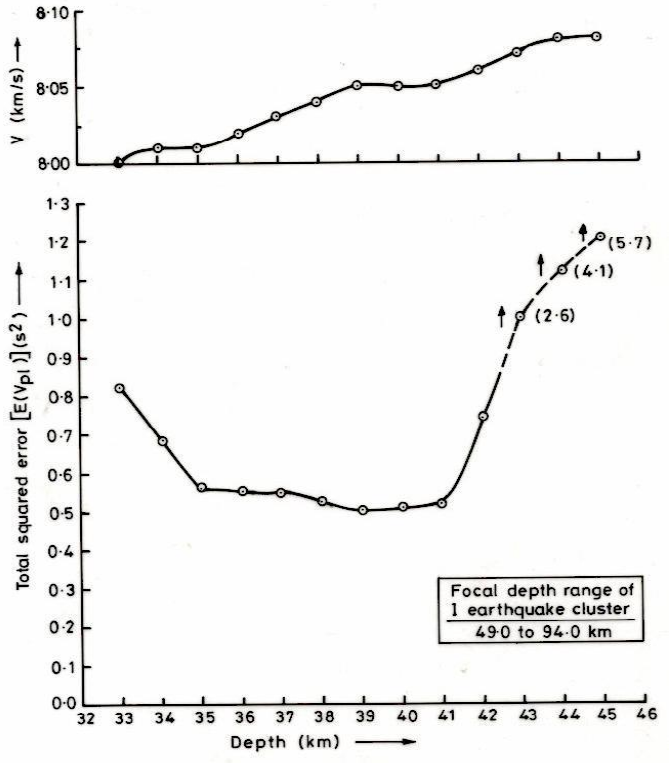

Figure 7. E (Vpl) and Vp for grid search using I earthquake cluster data. Depth on vertical axis for assumed depth of I interface.

above-mentioned computer program was used to estimate V_{pl} for a number of assumed values of depth of the top interface of the *l* th layer. In each case, the total squared error E (V_{pl}) of equation (1) was also computed. That value of depth was adopted for which the value of E (V_{pl}) was the least. The corresponding estimate of V_{pl} became the accepted value of V_p in the *l* th layer.

RESULTS

We now present the results of the exercise to interpret the observed travel times using the computer program and grid search algorithm just described.

Earthquake clusters

The clustering in focal depth of 22 earthquakes has been remarked already. We now formally call the seven earthquakes in the focal depth range of 49 to 94 km as the I cluster. Similarly, five earthquakes in the focal range of 117 to 142 km will be called the II earthquakes cluster. Finally, the 10 earthquakes in the focal depth range of 188 to 245 km will be referred to as the III earthquakes cluster.

Average V_{pl} in the crustal layer

The reason for assuming an average crustal layer has been given above. Here we justify the value of V_p adopted for it. According to Hirn et al. (1984), average of value of V_p in the crustal layer in the Himalaya is of the order of 6.3 km/s. However, for the Garhwal Himalaya, Sushil et al. (1987) observed from analysis of local data that the V_p in the second crustal layer has the relatively low value of 6.0 km/s. Hence, we adopt an average V_p of 6.2 km/s for the crustal layer in order to carry out the following modeling exercise.

Results on the assumption of a laterally uniform layering in the upper mantle between Hindu Kush and Garhwal Himalaya

Results of analyzing data for I earthquake cluster

Figure 7 is a display of E (V_{pl}) for different assumed thicknesses of the crustal layer while using the travel time data for the I earthquake cluster. It is seen that the minimum of E (V_{pl}) is a weak and broad one. But having setup the rule described above we have to conclude that a crustal thickness of 39 km and upper mantle V_{pl} of 8.05 km/s do yield the least total squared error.

Results of analyzing data for II earthquake cluster

Figure 8 is analogous to the preceding figure. However, the minimum in E (V_{pl}) is quite sharp and pronounced for a depth of 99 to 100 km for the top interface of the last layer in this case. It corresponds to a V_p of 8.37 km/s.

Results of analyzing data for III earthquake cluster

Figure 9 is the display of E (V_{pl}) using the data for the III earthquake cluster. It is observed that the minimum in E is again weak and there are three values namely 154, 164 and 176 km for the depth to the top of the last layer in this case. The V_p in the layer however is not significantly different from these three possible depths. In short, the wave velocity model obtained from this analysis may be summarized as in Table 5.

Taking account of local velocity structure in the Hindu Kush region

As mentioned above, Roceker's estimate of V_{pl} structure in the Hindu Kush region is also a multilayered one, though in subsequent refinements he has estimated lateral variation of V_p to occur in different layers. When we take account of this multilayered earth model, we are constrained to mesh it with the rest of the flat-layered earth model by putting a vertical boundary between them. Estimating the extant to which Roecker's model could

Table 5. Vp speed without local model of Roecker's.

Depth of boundaries from the Surface (Km)	P- wave velocity obtained (Km/s)
0	6.2 (assumed)
39	8.05
100	8.37
154 or 164 or 176	8.7 or 8.8 or 8.8

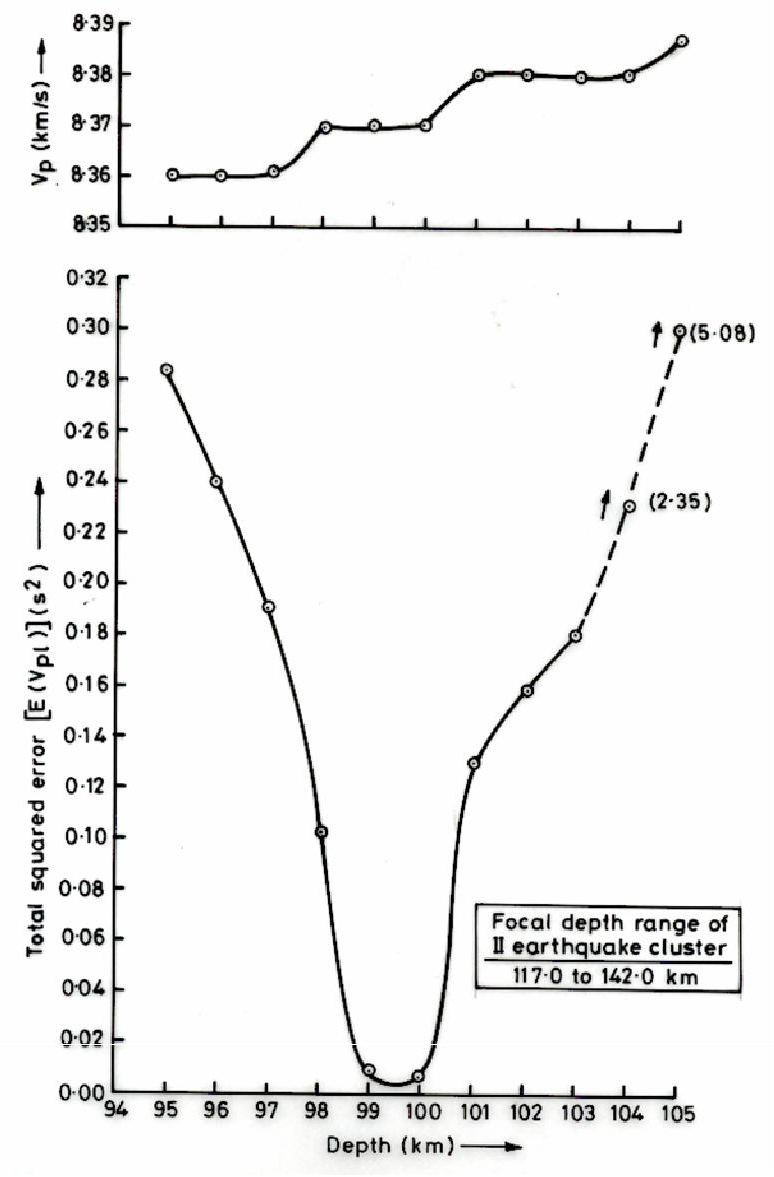

Figure 8. E (Vpl) and Vp for grid search using II earthquake cluster data. Depth on vertical axis for assumed depth of II interface.

exist along the ray path requires a somewhat arbitrary decision. Looking at the various maps and figures given by Roecker, we estimate that the boundary may be placed along the northeast-southwest striking Kunar fault in the Hindu Kush region (Figure 1).

Results

Figures 10, 11**,** and 12 correspond to Figures 7, 8 and 9 of the previous section. We conclude from Figure 10 that the crustal thickness should still be 39 km and V_p at the

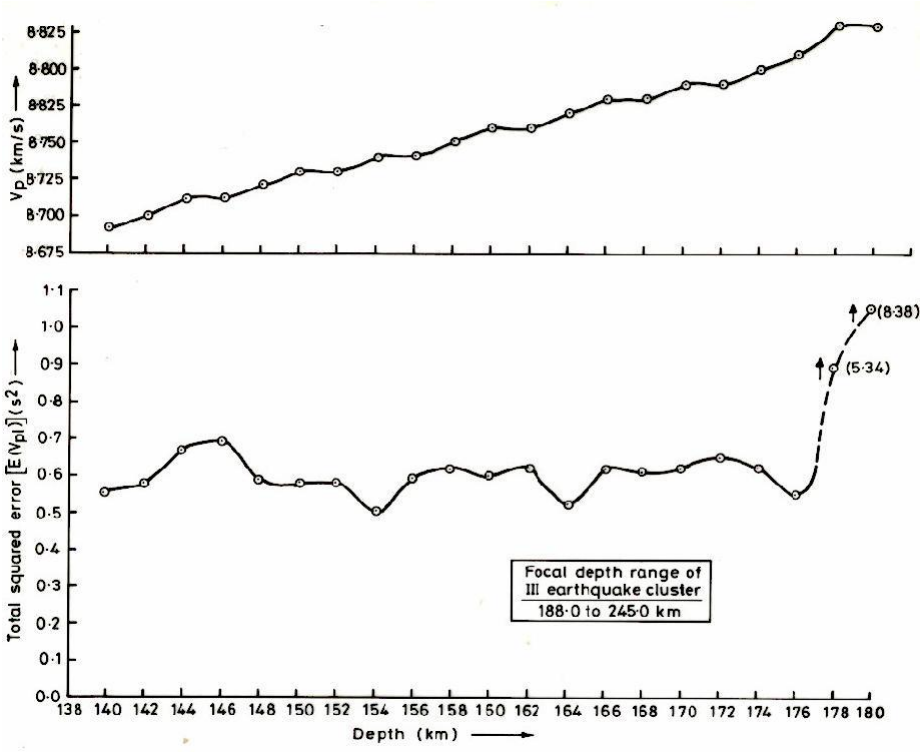

Figure 9. E (Vpl) and Vp for grid search using III earthquake cluster data. Depth on vertical axis for assumed depth of III interface.

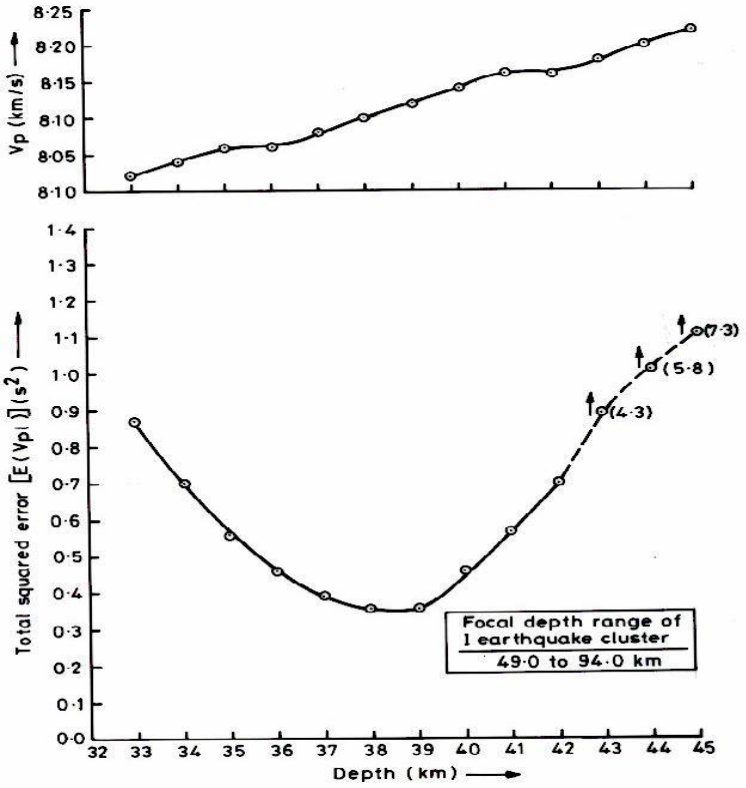

Figure 10. Same as Figure 7 but incorporating Roecker's model also for ray tracing.

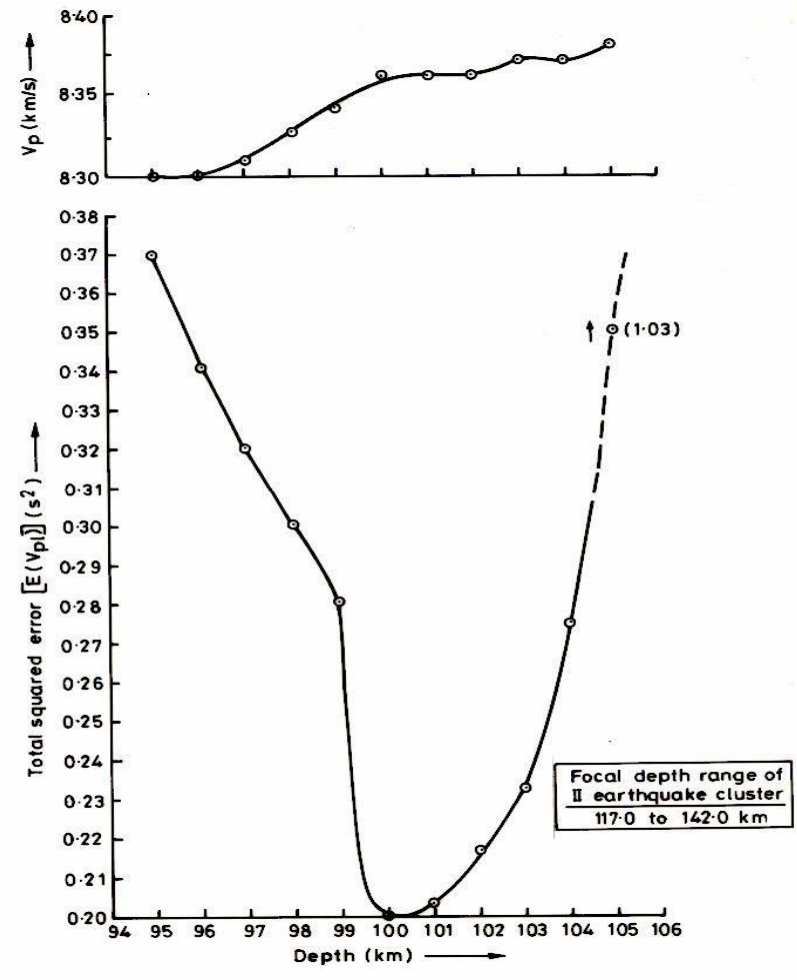

Figure 11. Same as Figure 8 but incorporating Roecker's model also for ray tracing.

Table 6. Vp speed when Roecker's model introduced at source zone.

Depth of boundaries from the Surface (Km)	P- wave velocity obtained (Km/s)
0	6.2 (assumed)
39	8.16
100	8.35
154 or 164 or 176	8.7 or 8.7 or 8.8

top of the upper mantle should be 8.16 km/s. The error function in Figure 12 shows that the layer boundary could be at 144, 158**,** and 174 km depth. The summary of the V_p structure is shown in Table 6.

A comparison of the information of Tables 5 and 6 is given in Table 7. We may conclude that the data from the I and II earthquake clusters give comparable results which can be considered as useful contributions of this exercise. The results for the III cluster loose in importance slightly because a clear-cut depth to the top of the relevant layer cannot be provided.

It is seen from Table 7 that taking account of the local structure in the Hindu Kush region has not altered the results significantly. This must be ascribed to the fact that the total lengths of the ray paths in the Hindu Kush structure are comparatively short. Still we have the satisfaction of having made the effort to take local structure in account.

Summary of the results

We may conclude from the above exercise for estimating V_p structure along the NW Himalaya that the V_p at the top of upper mantle is about 8.1 km/s. At a depth of 100 km from the surface, or 60 km from the Moho, an increase in V_p occurs to a value of 8.35 km/s approximately. Below that level there is a further increase in V_p value indicated from the data of the III earthquake cluster. However, the

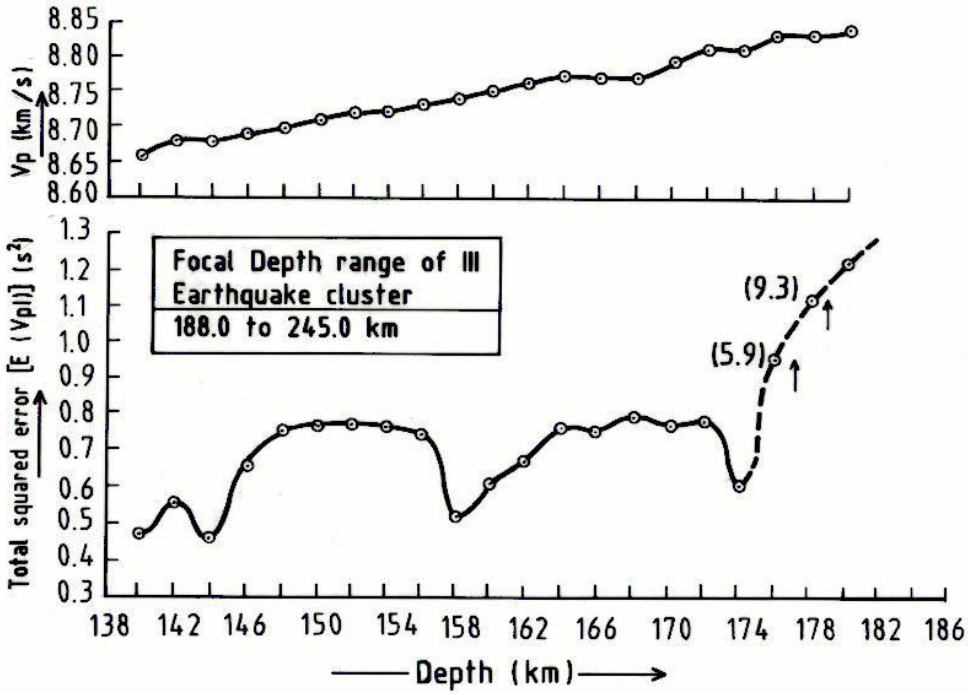

Figure 12. Same as Figure 9 but incorporating Roecker's model also for ray tracing.

Table 7. Final Table for the Vp determination between Hindu Kush and Garhwal Himalaya.

S/No.	Focal depth range of different cluster (km)	Depth of boundaries from surface (km)	P wave velocity obtained	
			Without local velocity structure (Km/s)	With local velocity structure (Km/s)
	0	6.2(assumed)	6.2(assumed)	6.2(assumed)
1.	49-94	39	8.05	8.16
2.	117-142	100	8.37	8.35
3.	188-245	154 or164 or 174	8.7 or 8.8 or 8.8	8.7 or 8.7 or 8.8

depth at which it could occur is uncertain over a depth range of 20 km. The level of V_p below that boundary would be about 8.7 km/s.

Discussion and Conclusion

Having obtained a V_p structure, it is natural to compare it with other determinations as far as possible. Of course, comparison with the results given in Table 2 is there. However, in our opinion a more useful comparison comes from the following remarks.

Ni and Barazangi (1983) studied body wave propagation in the India, Tibet, and Afghanistan using high quality WWSSN data. They estimated a value of 8.45 ± 0.08 km/s for P_n wave velocity in the Himalaya. This may be compared with our value of 8.1 km/s. The discrepancy between the two results is large and some explanation is required. All we can say is that when computing their values Ni and Barazangi had to use data in which the ray paths between earthquakes and recording stations were not strictly in the Himalaya. Whereas in our case, as seen from Figure 1, the great circles between the epicenters in the Hindu Kush and the recording stations in the Garhwal Himalaya do lie along the Himalaya over a very large fraction of their lengths. Hence, our determination is strictly for the Himalayan region.

Some DSS results for the Kashmir region are available in the literature. Figure 13 is a comparison of the geographic location of DSS profiles and our great circle. The most significant point in this connection is that an upper mantle V_p of 8.1 km/s is obtained again and this supports our determination considerably. Along the DSS profile, the Moho has wide depth variations. Towards the great

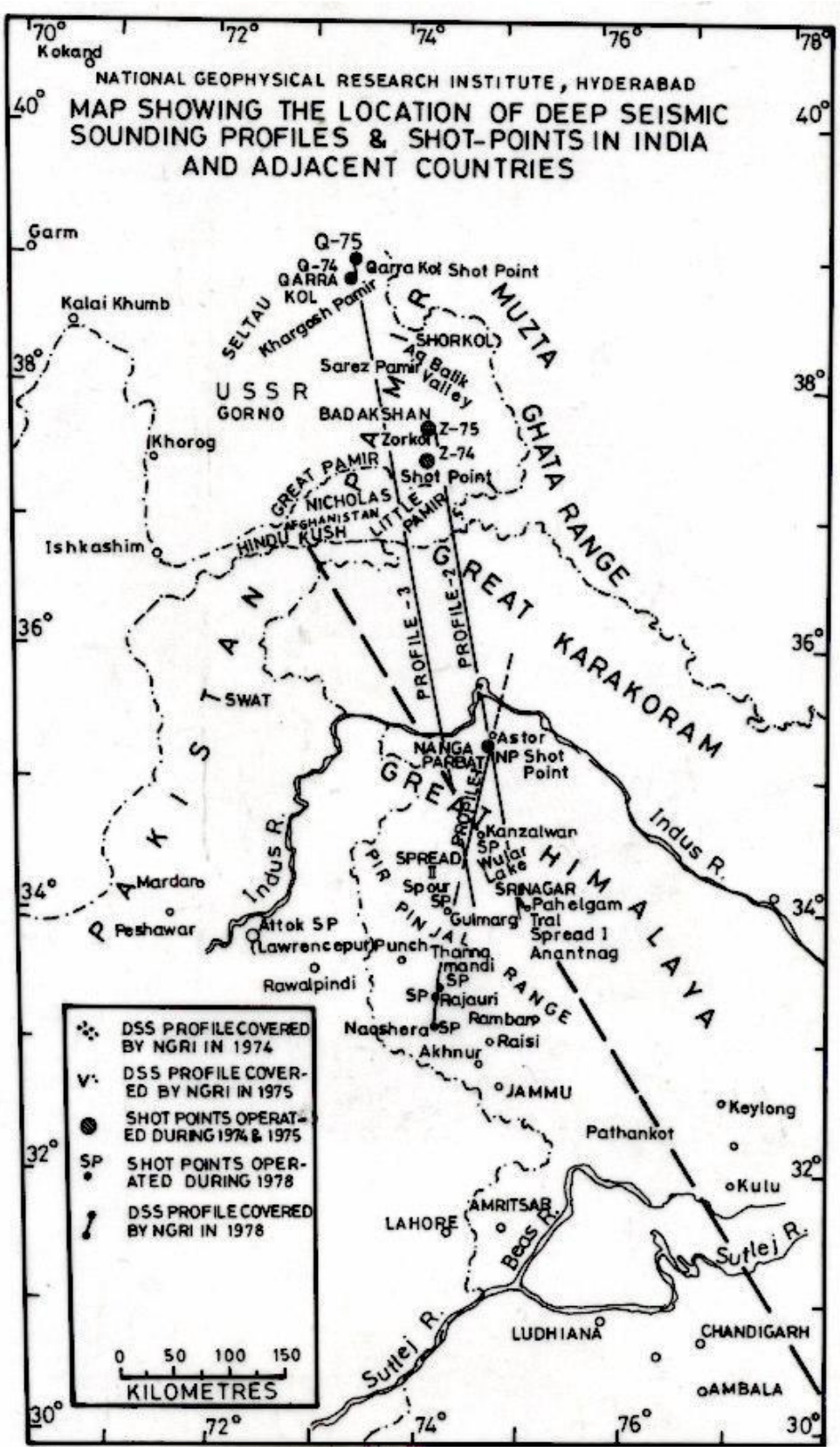

Figure 13. Relationship between DSS profiles (Kaila et al 1992) and the great circle between Hindu Kush epicenters and Garhwal stations. One great circle shown as representative of all the great circles.

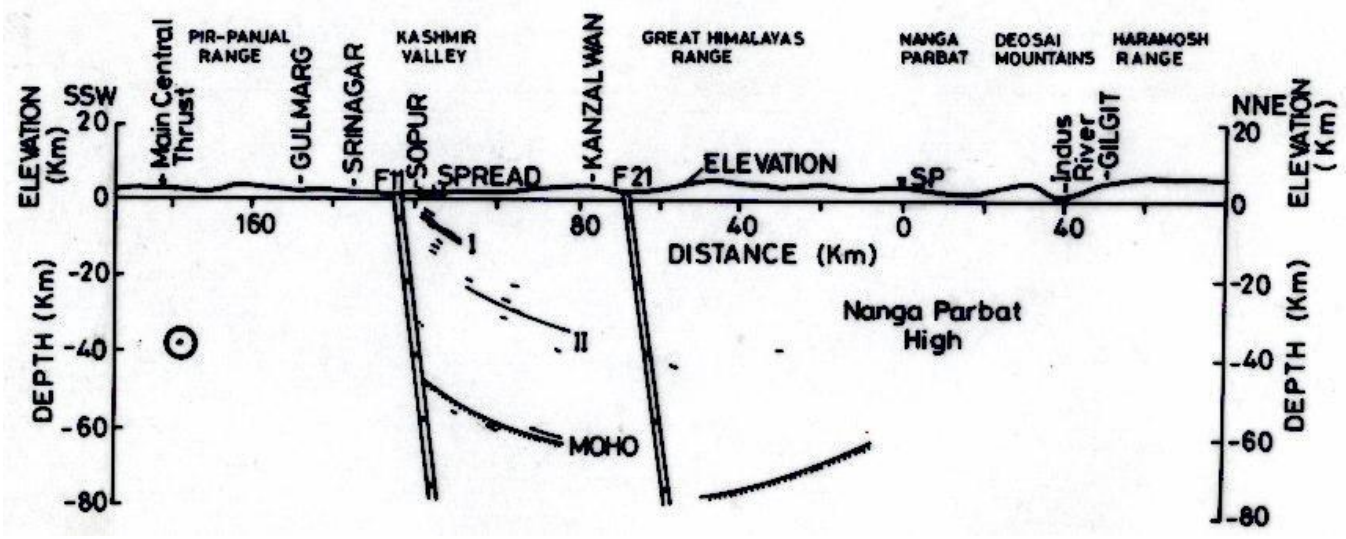

Figure 14. DSS results shown in depth section. Positions of great circles is also indicated.

circle of interest, the Moho appears to rise towards our estimated depth of 39 km (Figure 14).

ACKNOWLEDGEMENTS

Authors thank Prof. Tamao Sato, Hirosaki University, Japan for their valuable suggestions. Thanks to Director, Wadia Institute of Himalayan Geology, Dehra Dun, for providing all necessary facilities to complete this work. Special Thanks to the Department of Earth Science, I.I T. Roorkee, Roorkee for providing required MEQ Data. Memorable thanks to my wife Rama Sushil, my daughter Rashmi and son Siddharth for their cooperation at each step of this work.

REFERENCE

Aki K, Richards P (1980). Quantitative Seismology. Theory and Methods. W.H. Freeman, San Francisco.

Roecker SW (1982). Velocity structure of the Pamir-Hindu Kush region: Possible evidence of subducted crust. J. Geo. Res. 87 B2: 945-959.

Tandon AN (1967). Upper mantle seismic wave velocities in the Hindu Kush region, India. J. Met. Geophys. 18: 385-390.

Matveyeva MM, Lukk AA (1968). Estimates of the accuracy in constructing travel time curve for the Pamir-Hindu Kush zone and in the computer determination of the velocity profile in the upper mantle. Izv. Acad. Sci. U.S.S.R. Phys. Solid Earth, Engg. Transl. 8: 466-473.

Kaila KL, Krishna VG, Narain H (1969). Upper mantle velocity structure in the Hindu Kush region from travel time studies of deep earthquakes using a new analytical method. Bull. Seismol. Soc. Am. 59: 1949-1967.

Ram A, Mereu RF (1977). Lateral variations in upper mantle structure around India as obtained from Guaribidanur seismic array data. Geophys. J. R. Astr. Soc. 49: 87-114.

Bullen KE, Bolt BA (1985). Theory of seismology, Cambridge University press, Cambridge.

Shah PM (1973). Ray tracing in three dimensions. Geophysics 38(3): 600-604.

Sorerells GG, Crowley JB, Veith KF (1971). Methods for computing ray paths in complex geological structures. Bull. Seism. Soc. Am. 61(1): 27-53.

Chander R (1977). On tracing seismic rays with specified end points in layers of constant velocity and plane interfaces. Geophys. Prospect 35: 120-124.

Hirn A, Lapine JC, Jabert G, Sapin M, Wittlinger G, Xin XZ, Yuan GE, Jing WX, Wen TJ, Bai XS, Pandey MR, Tater J (1984). Crustal structure and variability of the Himalayan border of Tibet. Nature 307: 23-25.

Kumar Sushil, Chander R, Khattri KN (1987). Compressional wave velocity in the second crustal layer in Garhwal Himalaya. J. Assoc. Expl. Geophys. 8: 219-225.

Ni J, Barazangi M (1983). High frequency seismic wave propagation beneath and Indian Shield, Himalayan Arc, Tibetan Plateau and surrounding regions high uppermost mantle velocities and efficient S_n. Propagation beneath Tibet. Geophy. J. R. Astr. Soc. 72: 665-689.